Proceedings of the 14th
KACC, Octorber 1999

A Practical Approach to Mass Estimation of Loose Parts

Jung-Soo Kim° and Joon Lyou*
° Korea Atomic Energy Research Institute MMIS Team
P.O.Box. 105 Daeduk danji Taejeon 305-606, Korea
Tel. : 82-42-868-2924
Fax :82-42-868-8357
Email: kjs@nanum.kaeri.re.kr
* Dept. of Electronics Engineering, Chungnam National Univ.

Abstract

This paper is concerned with estimating the mass of a loose part in the steam generator of a nuclear power plant. Although there is the basic principle known as "Hertz Theory" for estimating mass and energy of a spherical part impacted on an infinite flat plate, the theory is not directly applicable because real plants do not comply with the underlying ideal assumptions. (Say, the steam generator is of a cylindrical and hemisphere shape.) In this work, a practical method is developed based on the basic theory and considering amplitude and energy attenuation effects. Actually, the impact waves propagating along the plate to the sensor locations become significantly different in shape and frequency spectrum from the original waveform due to the plate and surrounding conditions, distance attenuation and damping loss. To show the validity of the present mass estimation algorithm, it has been applied to the mock-up impact test data and also to real plant data. The results show better performance comparing to the conventional Hertz schemes.

1. Introduction

LPMS (Loose Part Monitoring System) is a diagnostic system that monitors the integrity of Nuclear Steam Supply System (NSSS) and analyzes the impact event caused by moving or loose parts. This system provides the necessary information for the operator's proper decision to maintain a reliable and safe nuclear power plant. The loose parts, metal pieces, are produced by being parted from the structure of the reactor coolant system (RCS) due to corrosion, fatigue, and friction between components in RCS and also by coming into RCS from the outside during the period of reactor test operation, refueling, and maintenance during overhaul. These loose parts are mixed with reactor coolant fluid, move with high velocity along RCS circuits, and generate collisions with RCS components. When a loose part strikes against component within the pressure boundary, an acoustic impact wave is produced and propagates along the pressure boundary. In order to detect the impact signal, conventional LPMS uses the accelerometer sensor installed on the outer surface of the pressure boundary of RCS components and announces an alarm when the detected impact signal exceeds a certain level which is pre-set by the operator. The sensors are usually installed on the probable places where loose parts may collect or exist such as the upper head of the reactor pressure vessel, hot chamber of the Steam Generator [1]. Fig.1 shows typical sensor locations, where the sensor locations are marked with a block circle.

In the existing LPMS, the alarm is triggered in the case where the measured signals exceed the signal threshold and the detected signal is recorded on magnetic tape. Later, experienced operators analyze the recorded data and determine whether the detected signal is an impact signal by a loose part or a noise signal. If they conclude that loose parts caused the signal, they evaluate the characteristic parameters such as impact location, energy, and mass. After the diagnosis process mentioned above is completed, the proper procedure required for maintaining the safe and reliable operation is performed. In the conventional diagnostic method in LPMS, the operators should have expert knowledge for diagnosing the impact signal in order to execute proper action. Moreover, it takes a long time to analyze the detected signal data and hence possibly fatal damage of components may occur during the analysis procedure. Therefore, it is very desirable that if the alarm is triggered by a loose part's impact, the detected signal is stored in the computer memory, the automatic diagnosis procedure is activated immediately, and the diagnostic results (such as location, mass, and energy of loose parts) are displayed on the operator's monitors.

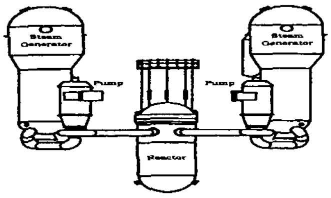

Fig.1. The typical sensor locations

Generally, two methods for mass estimation have been known: one is time series analysis and the other is frequency analysis. In the case of time series analysis, Hertz impact theory is used to determine the loose parts impact signal model and the equations for plate wave propagation are derived [2-4]. But the theory is not directly applied to real plants because of violations of the underlying ideal assumptions. For instance, the structure of a steam generator consists of two parts; the side is of cylindrical shape and upper & lower parts of hemisphere shape. The impact source is not the solid sphere. On the other hand, in using the frequency analysis [5-6], we should first change the impact (time) data to frequency data using Fast Fourier Transformations (FFT). From the frequency spectrum, we then find the characteristic frequency and estimate the mass referring to the look-up table. Fig. 2 shows a sample of converting to frequency domain. In the figure, we can not exactly distinguish the characteristic frequency from those of sensor resonance and background noise.

In this work, an automatic diagnosis algorithm for estimating the mass of a loose part is developed using time domain data and modifying the basic theory for its practical application. The present scheme is applied to the impact data of mock-up facility and real steam generator, and the experimental result show that it is performs better performance than the conventional method.

2. Hertz Impact Theory[1]

The Hertz theory describes the impact of a solid sphere on a metal infinite plate. This theory is based on the assumption that the principal response of the plate is a bending wave of half period equal to the duration of the plate, and the form of impact signal. Experimental results support this theory when the diameter of the sphere is not large comparing to the thickness of the plate and when the velocity of impact is sufficiently small to avoid plastic deformation [1]. Fig. 3 shows the sinusoidal waveform of the impact signal, when impacting the infinite plate by the solid sphere

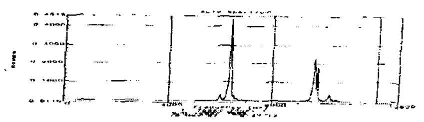

Fig.2 Example of the frequency spectrum of an impact signal

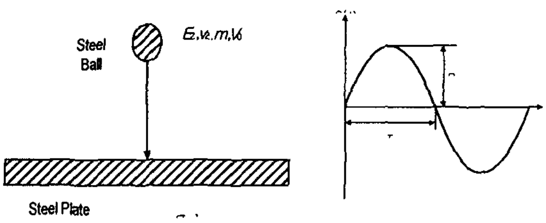

Fig.3. Clash test and the impact waveform

Under the assumption of sine waveform, the maximum amplitude (D_{max}) of the displacement and the *contact time* (T_d) *of solid sphere during contacting* are as follows:

$$D_{max} = K_h (mV_0^2)^{0.4} R^{-0.2} \quad (1)$$

$$T_d = 2.94 \frac{D_{max}}{V_0} \quad (2)$$

$$\text{with } K_h = \left[\frac{15}{16}\left(\frac{1-\nu_1^2}{E_1} - \frac{1-\nu_2^2}{E_2}\right)\right]^{0.4},$$

where m: the mass of the sphere, R: the radius of the sphere, ν_1 and E_1: Poisson's ratio and Young's Modulus for the plate, ν_2 and E_2: Poisson's ratio and Young's Modulus for the sphere and V_0: the initial velocity of the sphere. In (2), *it is noted that the Hertz theory* defines the relationship between V_0 and T_d.

Elastic or near-elastic impacts between metal objects and a metal plate are generally characterized by the contact force time history that is very close to the *half-sine function* [3]. The acceleration of the impacting object during contact is proportional to this force through the Newton's second law of motion. This relationship and the maximum displacement predicted by Hertz theory can be used to obtain the equation of motion of the impacting object during the contact time. Eqns. (3), (4) and (5) represent the displacement, the velocity and the acceleration of impact, respectively.

$$D(t) = D_{max} \sin\left(\frac{\pi}{T_d} t\right) \quad (3)$$

$$D'(t) = V(t) = \frac{\pi}{T_d} D_{max} \cos\left(\frac{\pi}{T_d} t\right) \quad (4)$$

$$D''(t) = A(t) = -\left(\frac{\pi}{T_d}\right)^2 D_{max} \sin\left(\frac{\pi}{T_d} t\right) \quad (5)$$

And using (5), the contact force time history is given by

$$F(t) = m\,A(t) \qquad 0 < t < t_d \quad (6)$$

From (4), the maximum velocity would be

$$V_{max} = V(0) = V_0 = \pi/T_d\, D_{max} \quad (7)$$

In other words, the contact time T_d is related with the initial velocity V_0 as

$$T_d = \pi\, D_{max} / V_0 \quad (8)$$

Comparing (2) with (8), (2) differs from (8) by a factor of $\pi/2.94(\cong 1.6)$. The exact half-sine interpretation of the impact displacement does not exactly match the Hertz theory equation, instead they provide the comparable result.

3. Consideration of the attenuation effects

3.1 Wave propagation along the plate

Solutions for the propagation of two dimensional waves away from a localized force were given by Lamb[7]. *The solution for propagating wave shape,* after normalized to the displacement amplitude obtained from the Hertz theory, can be used to calculate the plate surface acceleration wave and magnitude as a function of impacting object mass and velocity. This is not easily done due to the nonlinear characteristic of the equation.

An alternative method to relate impact properties to the plate wave acceleration is to assume that the acceleration wave consists primarily of a few half periods at the frequency 1.6 times more than that of the observed actual signals. And the magnitude of this signal is set to the plate acceleration waveform. The force and the acceleration at the sphere's point are related by

$$A_{ball} = F_{max} / m = k_h^{-1} m^{-0.4} V_0^{1.3} R^{0.2} \quad (9)$$

Redefining into the plate's point, (9) becomes

$$A_{plate} = F_{max} / M_{eff} \quad (10)$$

where F_{max} : *the maximum impact force and* M_{eff}: an effective mass of the plate. Note that the same force term F_{max} is used in (9) and (10), while the mass term, m, in (9) is replaced by M_{eff} in (10). The effective mass of the plate volume responding during the contact time is given by

$$M_{eff} = \pi \ (C_b \ T_d)^2 \ h \ \rho_{steel}$$

where C_b : the phase velocity of a bending wave in a steel plate = C_{LI} ($1.8hf_a$ / C_{LI} + $4.5hf_a)^{0.5}$, C_{LI} : 5,270 m/sec, T_d: contact time, h : the plate thickness, ρ_{steel} : the density of the plate. See Fig. 4.

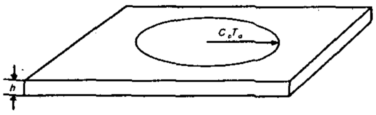

Fig.4. The effective mass of the plate

3.2 Distance attenuation and damping loss

From (11), we calculate the mass estimation in the case that the impact point is equal to the installed sensor position. But, in general, since the sensor position does not coincide with the impact point, it is necessary to compensate for damping and distance attenuation for the plate. A transverse impact against a plate excited a cylindrical wave whose radius increases with time as the wave propagates away from the impact point. The amplitude of this wave decreases as a function of the distance due to the increasing area covered by the wave and energy losses, referred to as damping. These attenuation effects can be combined to define the wave amplitude as a function of distance.

The distance attenuation occurs when the impact signal is propagating from impact point to sensor location. The characteristic of the impact signal can be expressed as many values of kr (k is the wave number and r is the distance) with the asymptotic approximations for the Hankel function. Eq. (11) expresses the relationship between the distance and the amplitude. That is, the decrease in amplitude of a plate's bending wave is proportional to an increase in distance from the impact source.

$$D(r) = D_0 [H_0(kr) - H_0(-jkr)] \qquad (11)$$

where D(r): the displacement amplitude at distance r from the impact, D_0: the displacement amplitude at the point of impact, k: the wave number($2\pi f / D_0$), H_0 : the Hankel function of the 2nd kind, $H_0(kr) = 2j/\pi \ln (kr)$ {|kr| <<1}, $H_0(kr) = (2kr/\pi)^{0.5} \exp (-j(x - \pi/4))$ {|kr| >>1}.

Impact wave attenuation during propagation also occurs due to the internal energy dissipation along the plate and the radiation energy to the surrounding fluids. Eq. (12) expresses this type of loss for bending waves.

$$D(r) = D_0 e^{-\left(\frac{\pi \eta f}{C_g}\right) r} \qquad (12)$$

where D_0 : the initial amplitude, η : the loss factor, f : the frequency of interest, γ : the distance traveled and C_g : the bending wave group velocity.

$$C_g = \frac{3.6 C_{LI}^2 h f}{C_b (C_{LI} + 9 h f)}$$

$$\eta = \frac{\rho_0 c_0}{2 \pi f \rho_s h} \times \frac{M_f}{\sqrt{M_f^2 - 1}} .$$

4. Experimental Result and Discussions

4.1 Mock-up experiment

Before applying the developed algorithm to the impact sources, we gathered the impact signals from the mock-up system. Fig. 5 shows the reactor mockup made of stainless steel whose size is scaled down to 1/7 and thickness is 10mm. Main components installed are structure supports, feed-water and drain components and accelerometers. 18 sensors (accelerometers) are attached on the side, at intervals of 60 ° and 14 sensors are attached on the upper head and 14 sensors on the lower head. Fig. 6 shows the mass estimation window. The input parameters needed are the distance between sensor and impact, the initial half period of impact wave and the maximum amplitude at initial period. Fig. 7 shows the flow of the developed mass estimation algorithm. From the flowchart, we see that the basic algorithm of Hertz theory is modified by revising it through trial and error and many tests. To be specific, we branch the half period into three paths. Table 1 summarizes the mass estimation results after running the developed algorithm in the case where there is an *impact at 30cm, 70 cm, 110 cm away from the sensor* using an impact ball at the height of 6 cm. The sphere mass was 30.5g and the diameter was 1.9cm. Tests were conducted three times at each and every distance. The average error rate is 16 % for mass estimation.

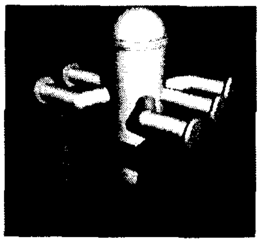

Fig.5. Reactor Mockup

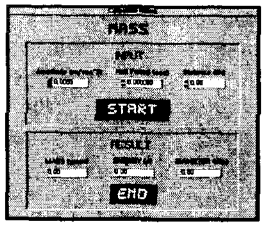

Fig.6. Display Window

Table 1. Test results (actual mass : 30.5g and actual *diameter : 1.9 cm)*

Distance-frequency	Mass(g)	Diameter (cm)
30-1	36.75	2.0746
30-2	33.24	2.0065
30-3	39.85	2.1314
70-1	34.11	2.0238
70-2	36.15	2.0634
70-3	36.70	2.0737
110-1	36.00	2.0605
110-2	31.30	1.9666
110-3	35.38	2.0485

4.2 Application to the real impact data

Figs. 8 & 9 demonstrates the recorded impact signals with the sampling time 3 * 10^{-5} sec from the accelerometer of the steam generator. Two accelerometers are installed in the steam generator : one at the primary side and the other at the secondary side. And there are three steam generators. The radius of steam generator is 2.115m and the normal flow velocity was 7.8 m/sec and the flow velocity at hot chamber was 1.23 m/sec. The distance between the primary and the secondary is 1.5m apart. The impact events occurred were three. From Figs. 8 & 9, we observe that the impact bursts show up on the two points 755 and 757 which mean the sensor numbers, and 754 is affected by the impact signal of 755. Fig. 9 enlarges a portion of Fig. 8 on the extended time scale. And Figs. 10 emphasize the burst signals of Fig 9. Based on these data, we can estimate the impact location [8] and other input parameters: the distance between sensor and impact positions is about 1.9m, the maximum amplitude about139.763 m/sec, the initial half period about 75.37 μsec. Now, the developed algorithm guesses the mass about 500 – 600 gram. After the three times trials, Table 2 shows the results of our analysis are nearly the same as those of the expert signal analysis-company. Even if the estimated results are more or less different from the actual value, our results are thought to be good enough taking the actual environment in account (different background noise level, the impact source is not a sphere and so on). Later, it was found that impact source was a bolt and nut.

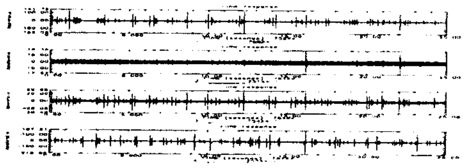

Fig. 8 Actual impact signal from plant

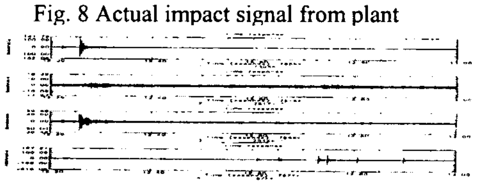

Fig.9. Enlarged portion of Fig.8.

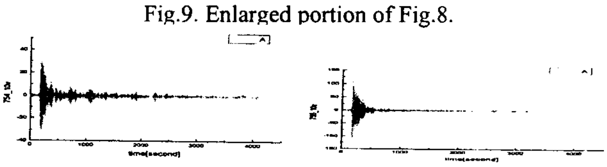

(a) (b)

Fig.10. Burst signal s : (a) at 754 (b) 755

Table 2. Comparison of the estimated and actual mass

Event Date-Frequency	Present Estimation result	Foreign company estimation result	Actual Mass
1997 – 1	A:500-600g B: 300-400g	A: 1.5 Pound B : 1 pound	A: about 200g B: about 100g
1999 – 1	39 - 42g	N/A	N/A
1999 – 2	75 – 82 g	N/A	76.6g

5. Concluding Remarks

In the conventional LPMS, the operators should have expert knowledge for analyzing the impact signal data and mass estimation. In this work, we have developed an automatic mass estimation algorithm and applied to the reactor mockup and the actual plant impact signal. In the case of the mockup tests, the average error rate between the estimated value and actual value was comparatively small due to noise-free environment. But, the error rates for the real signal case appears more than the former case, because the actual plant include a high level of background noise(damping factor and the material's attenuation) and the impact source is of arbitrary shape.

If we use the developed algorithm in an existing plant or a new plant, this algorithm would provide the more accurate mass-estimated information to the operator contributing to the safety and the prevention of accidents in a NPP. Further studies of interest are to introduce the new technology such as neural network or wavelet transformation.

Reference

[1] Mayo C. W. et al, Loose Parts Monitoring System Improvements, EPRI NP-5743, Final Report, March 1988.

[2] Joseph A. Thie, Power Reactor Noise, American Nuclear Society, 1981.

[3] Charles W. Mayo, "Loose part signal theory", Progress in Nuclear Energy, Vol. 15, pp. 535-543, 1985.

[4] B. J. Olma, " Source Location and mass Estimation in Loose Parts Monitoring of mass estimation algorithm LWRs." Progress in Nuclear Energy, Vol. 15, 1985.

[5] T. Tsunoda, et al, " Studies on the Loose part Evaluation Technique", Progress in Nuclear Energy, Vol. 15, 1985.

[6] B. J. Olma and B. Schutz, " Advanced Burst Processing Methods in Loose Parts Monitoring" SMORN V, Progress in Nuclear Energy, Vol. 21, pp. 525-535, 1987.

[7] H. Lamb, "On Wave-Propagation in Two Dimensions", Proceedings of the London Mathematical Society, Vol. 35, 1902, pp. 141-161.

[8] J.S.Kim and J.Lyou," An Automatic Diagnosis Method for Impact Location Estimation", in Proceeding KACC, International Session, pp. 295-300, Oct. 1998.

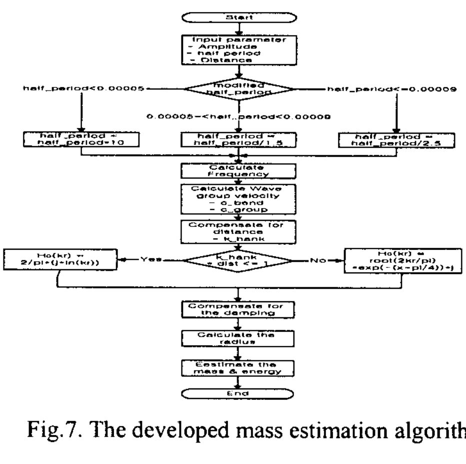

Fig.7. The developed mass estimation algorithm